

2016

Modelling And Simulation Of A R744 Based Air Conditioning Unit

Mihir Mouchum Hazarika
IIT KHARAGPUR, India, mihirbesu2011@gmail.com

Maddali Ramgopal
IIT KHARAGPUR, India, ramg@mech.iitkgp.ernet.in

Souvik Bhattacharyya
IIT KHARAGPUR, India, souvik.iit@gmail.com

Follow this and additional works at: <http://docs.lib.purdue.edu/iracc>

Hazarika, Mihir Mouchum; Ramgopal, Maddali; and Bhattacharyya, Souvik, "Modelling And Simulation Of A R744 Based Air Conditioning Unit" (2016). *International Refrigeration and Air Conditioning Conference*. Paper 1615.
<http://docs.lib.purdue.edu/iracc/1615>

This document has been made available through Purdue e-Pubs, a service of the Purdue University Libraries. Please contact epubs@purdue.edu for additional information.

Complete proceedings may be acquired in print and on CD-ROM directly from the Ray W. Herrick Laboratories at <https://engineering.purdue.edu/Herrick/Events/orderlit.html>

Modelling and Simulation of a R744 based Air Conditioning Unit

Mihir Mouchum HAZARIKA^{1*}, Maddali RAMGOPAL², Souvik BHATTACHARYYA³

^{1,2,3}IIT Kharagpur, Department of Mechanical Engineering,
Kharagpur, India

¹E-mail: mihirbesu2011@gmail.com

²E-mail: ramg@mech.iitkgp.ernet.in

³E-mail: souvik.iit@gmail.com

* Corresponding Author

ABSTRACT

Studies show that the performance of transcritical R744 systems is highly sensitive to the high side pressure in the gas cooler. Hence use of appropriate strategy to control the high side pressure is essential to extract the best performance from these systems. In the present study, a R744 based air conditioning cycle with two expansion valves is considered for proper control of high side pressure and quality of refrigerant at evaporator exit. A system simulation model is developed for this cycle considering detailed model for each component. Both the gas cooler and evaporator considered here are crossflow heat exchangers with spiral fin and tube geometry. A discretized approach is considered for developing the models for gas cooler as well as evaporator. Elemental *Log Mean Temperature Difference* (LMTD) and *Log Mean Enthalpy Difference* (LMED) approaches are used to model the gas cooler and evaporator, respectively (Yin et al., 2001a; Threlkeld, 1970a). An empirical model proposed by Brown et al. (2002a) is considered for modelling the reciprocating compressor. Expansion process in the valves is assumed to be isenthalpic. Using the developed model, the effects of variation of various important environmental parameters on system performance is analyzed. From the results obtained, optimum operating conditions are identified for which the system attains maximum COP. It is expected that this study will be beneficial in the design and development of suitable control strategies for small air conditioners based on transcritical CO₂ cycles.

1. INTRODUCTION

With the growing interest in CO₂ as a refrigerant, research efforts on CO₂ based refrigeration system are increasing exponentially over the past few years, the primary goal of which is to make CO₂ based systems competitive in today's market. It is well known that as the critical temperature of CO₂ is low (31.1°C), for hot climatic conditions, the heat rejection process has to be carried out under supercritical conditions for CO₂ based air conditioning systems, while the heat extraction is subcritical. Lorentzen and Pettersen (1993) first demonstrated a transcritical CO₂ based mobile air conditioner where heat rejection process is carried out at supercritical pressure. In the supercritical zone, pressure becomes independent of temperature. Furthermore, the isotherm characteristic is unique in the supercritical zone. As a result, performance of the system is different at different pressures for the same exit temperature at gas cooler, and for a particular gas cooler exit temperature, highest system COP is achievable only for a specific pressure in the gas cooler. Hence an appropriately smart strategy is required for controlling the high side pressure in the gas cooler to extract the maximum system COP.

For conventional air conditioning systems with synthetic refrigerant, a throttle valve is used as an expansion device. Depending upon the type, the valve maintains the required low side pressures and mass flow rate through the system. However, for transcritical CO₂ based air conditioning systems with one expansion valve, it is not possible to optimally control the high side pressure as well as refrigerant flow rate. Use of two expansion valves in series with a receiver in between is considered to be more reliable for control of high side pressure and superheat at the evaporator exit. This particular control strategy has been analyzed by Casson et al. (2003a), Zhang et al. (2010),

Boccardi et al. (2013), and Peñarrocha et al. (2014). They have suggested that use of two expansion valves enhances the controllability and hence performance of the system. However, majority of the reported studies still consider only a single expansion device.

In the present study, a R744 based air conditioning cycle with two expansion valves is considered. Based on the proposed cycle, a comprehensive mathematical model is developed considering fin-and-tube heat exchangers. Design dimensions for different components are predicted using the developed model. Optimum operating parameters are identified from the results of numerical simulations. Moreover, the effects of various important environmental parameters on system performance are analyzed. It is expected that the developed model will be helpful toward better understanding of transcritical behavior of the system.

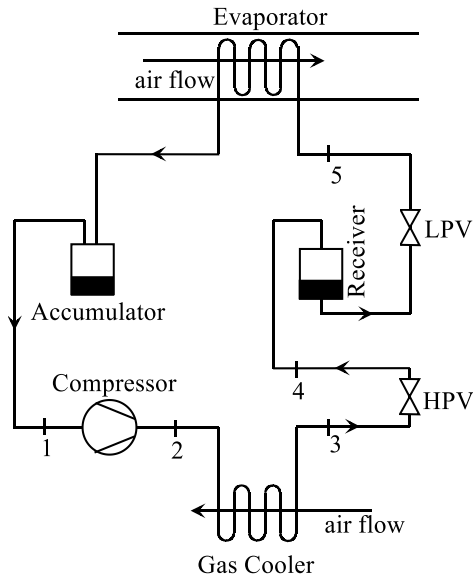


Figure 1: Schematic of the R744 based air conditioning unit

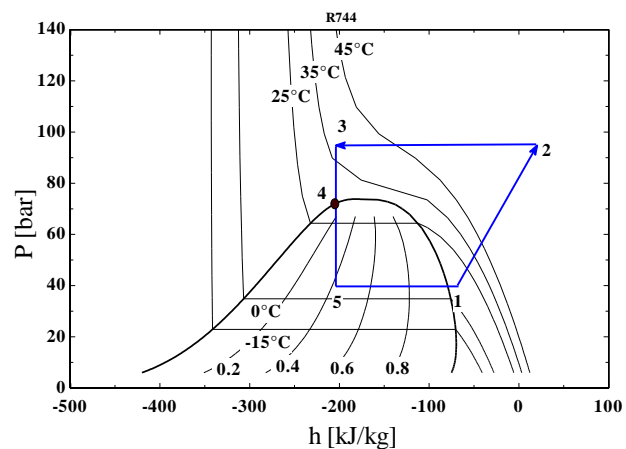


Figure 2: p - h diagram of the R744 based air conditioning unit

2. SYSTEM DESCRIPTION

The cycle schematic and p - h diagram of the cycle are shown in figures 1 and 2, respectively. As shown, the main components of the system are: compressor, gas cooler, a differential valve as a high pressure expansion valve (HPV), receiver, a thermostatic expansion valve as a low pressure expansion valve (LPV), evaporator, and accumulator. High pressure gas leaving the gas cooler is expanded first in the HPV. At the exit of first stage of expansion, the fluid becomes saturated liquid and enters the receiver. The refrigerant is then sent to the evaporator through LPV. The superheated vapor that leaves the evaporator is compressed in the compressor. The high temperature and high pressure refrigerant leaving the compressor is then sent to the gas cooler for heat rejection.

3. MATHEMATICAL MODEL

The present model for complete simulation of the transcritical CO_2 based air conditioning unit is developed based on a few assumptions. Using the developed model, numerical simulations are carried out to investigate the performance of the system with two expansion valves. A brief description of the assumptions considered as well as the mathematical model of the compressor, gas cooler, expansion valves and evaporator is presented in this section.

3.1 Compressor

In the present study, a semi empirical model is developed for the compressor using correlations proposed by Brown et al. (2002b). For volumetric efficiency and isentropic efficiency of the compressor, correlations are expressed in the following form (Brown et al., 2002c):

$$\eta_v = 0.8263 \left[1 - 0.09604 \times \left(r_p^{\frac{1}{\gamma}} - 1 \right) \right] \quad (1)$$

$$\eta_{is} = 0.9343 - 0.04478 \times r_p = \frac{h_{ex, is} - h_{in}}{h_{ex} - h_{in}} \quad (2)$$

Mass flow rate of refrigerant through the compressor is then calculated from:

$$\dot{m}_{ref} = \eta_v \rho_{in} (PD \times RPS) \quad (3)$$

3.2 Gas cooler

Elbel et al. (2014) have suggested that counter cross flow is the most suitable configuration for fin and tube gas cooler used in R744 based systems. To avoid heat conduction along fin surface, they suggested use of cut fins for heat exchangers in R744 based systems. For heat exchangers with spiral fin and tube configuration, there is no contact between fins of adjacent tubes, and therefore conduction of heat does not occur among fins of adjacent tubes. Besides it is easier to fabricate heat exchangers with spiral fin and tube configuration and is thus the choice the counter cross flow gas cooler used in the present R744 based system.

To design this counter cross flow gas cooler, a discretized approach has been adopted. The assumptions considered for designing the gas cooler are:

- The entire heat exchanger is divided into three dimensional array of nodes.
- In the three dimensional configuration, nodes are arranged by using i, j and k co-ordinates.
- As counter cross flow arrangement is considered for the gas cooler, calculation is carried out by an iterative procedure. Calculation is first started from refrigerant exit based on some guessed value of pressure and temperature at the exit. Marching is then started node by node from refrigerant exit to refrigerant inlet. At the end of this march, pressure and temperature are obtained at refrigerant inlet. These pressure and temperature at refrigerant inlet are then matched with actual condition by iterative procedure.

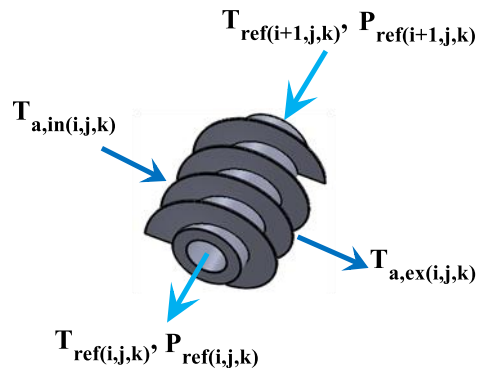


Figure 3: Isometric view of an elementary node of the gas cooler

3.2.1 Governing equations for each node: An elementary node is shown in figure 3. The procedure proposed by Yin et al. (2001b) is adopted here for calculating the heat transfer rate for each elementary node. Refrigerant side conservation equations are expressed in the following form:

$$Q_{node} = \dot{m}_{ref} (h_{i+1,j,k} - h_{i,j,k}) \quad (4)$$

$$Q_{node} = \alpha_{ref} a_{ref} LMTD_{ref} \quad (5)$$

where,

$$LMTD_{ref} = \frac{(T_{ref(i+1,j,k)} - T_{s(i,j,k)}) - (T_{ref(i,j,k)} - T_{s(i,j,k)})}{\ln \left(\frac{T_{ref(i+1,j,k)} - T_{s(i,j,k)}}{T_{ref(i,j,k)} - T_{s(i,j,k)}} \right)} \quad (6)$$

Pressure drop due to friction is calculated as:

$$P_{ref(i+1,j,k)} - P_{ref(i,j,k)} = \Delta P_f = f \frac{G^2 \times dL}{2 \times \rho \times d_i} \quad (7)$$

Air side conservation equations are expressed as:

$$Q_{node} = m_a C_{pa} (T_{a,ex(i,j,k)} - T_{a,in(i,j,k)}) \quad (8)$$

$$Q_{node} = \alpha_a \eta_o a_{node} LMTD_a \quad (9)$$

$$LMTD_a = \frac{(T_{s(i,j,k)} - T_{a,in(i,j,k)}) - (T_{s(i,j,k)} - T_{a,ex(i,j,k)})}{\ln \left(\frac{T_{s(i,j,k)} - T_{a,in(i,j,k)}}{T_{s(i,j,k)} - T_{a,ex(i,j,k)}} \right)} \quad (10)$$

where,

The correlation proposed by Pongsoi et al. (2013) has been used for calculating air side heat transfer coefficient and pressure drop. To calculate the heat transfer coefficient for supercritical in-tube carbon dioxide cooling, the correlation proposed by Pitla et al. (2002a) is used.

3.3 Expansion valves

The expansion processes in the expansion valves are considered as purely isenthalpic and are modelled as, $h_{in} = h_{ex}$. First stage of expansion is carried out using a differential valve, while the second stage of expansion is carried out using a thermostatic expansion valve. The differential valve is capable of maintaining the desired gas cooler pressure with desired pressure drop after first stage of expansion. Pressure drop across the differential valve is maintained in such a way that the fluid at the exit of first stage of expansion is in saturated liquid state (Casson et al., 2003b). In the second stage of expansion, the thermostatic expansion valve controls the refrigerant charge to produce the desired amount of superheat at evaporator exit. In between the two expansion valves, a receiver is placed. The receiver supplies required amount of charge to the evaporator as charge requirement varies for different operating conditions.

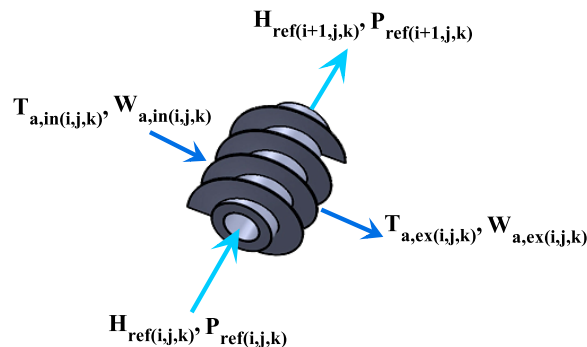


Figure 4: Isometric view of an elementary node of evaporator

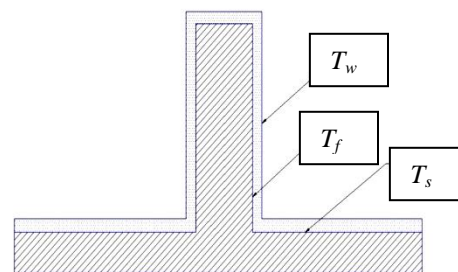


Figure 5: Sectional view of an elementary node of evaporator with water film forming on surface

3.4 Evaporator

Cross flow spiral fin and tube configuration has been chosen for the evaporator. Similar to the gas cooler, a discretized node by node approach has been used for designing the evaporator. Based on the state of refrigerant, the cooling coil of the evaporator is divided into two different zones: (a) two-phase zone and (b) single phase vapor zone. Condensation occurs on the external surface of cooling coil of the evaporator. Therefore each zone has been further subdivided based on the occurrence of condensation as (a) wet node and (b) dry node. During condensation, heat as well as mass transfer takes place on the external surface of the cooling coil. To incorporate the mass transfer effects, the method proposed by Threlkeld (1970b) has been adopted in the present analysis.

3.4.1 Governing equations for each node: For the coil surface for which condensation takes place, total heat transfer rate (sensible and latent) is calculated using the method proposed by Threlkeld (1970c). Isometric view and sectional view of an elementary node are shown in figure 4 and figure 5 respectively. ' T_w ' is the mean temperature of water film formed on the coil surface. ' T_f ' and ' T_s ' are mean temperatures of fin surface and tube surface, respectively.

For air side, heat transfer takes place from bare tube surface as well as from fin surface. Air side heat transfer rate can be expressed as (Threlkeld, 1970d):

$$\begin{aligned} dQ_{node} &= dQ_s + dQ_f = \left(\frac{\alpha_{o,w} a_s}{b_w} \right) \times (h - h_s) + \left(\frac{\alpha_{o,w} a_f}{b_w} \right) \times (h - h_f) \\ &= \left(\frac{\alpha_{o,w} a_s}{b_w} \right) \times (h - h_s) + \left(\frac{\alpha_{o,w} a_f \eta_f}{b_w} \right) \times (h - h_s) = \left(\frac{\alpha_{o,w}}{b_w} \right) \times (a_s + a_f \eta_f) \times (h - h_s) \quad (11) \\ &= \left(\frac{\alpha_{o,w} \eta_o a_{node}}{b_w} \right) \times (h - h_s) \end{aligned}$$

where ' b_w ' is slope of saturated air enthalpy evaluated at mean temperature of water film (T_w),

and

$$\alpha_{o,w} = \frac{1}{\left(\frac{C_{p,a}}{b_w \alpha_o} + \frac{y_w}{k_w} \right)} \quad (12)$$

For refrigerant side, heat transfer rate can be expressed as (Threlkeld, 1970e):

$$dQ_{node} = \alpha_i a_i (T_s - T_{ref}) = \frac{\alpha_i a_i}{b_{ref}} \times (h_s - h_{ref}) \quad (13)$$

where,

$$b_{ref} = \frac{(h_s - h_{ref})}{(T_s - T_{ref})} \quad (14)$$

Equating air side and refrigerant side heat transfer rate:

$$\begin{aligned} dQ_{node} &= \left(\frac{\alpha_{o,w} \eta_o a_{node}}{b_w} \right) \times (h - h_s) = \frac{\alpha_i a_{ref}}{b_{ref}} \times (h_s - h_{ref}) = \left(\frac{1}{\frac{b_w}{\alpha_{o,w} \eta_o a_{node}} + \frac{b_{ref}}{\alpha_i a_{ref}}} \right) \times (h - h_{ref}) \quad (15) \\ &= U_o a_{node} \times (\Delta h) \end{aligned}$$

where, $U_o = \left(\frac{1}{\frac{b_w}{\alpha_{o,w} \eta_o} + \frac{b_{ref} a_{node}}{\alpha_i a_{ref}}} \right)$ (16)

In the above expression, ' Δh ' is arithmetic enthalpy difference between mean air enthalpy ' h ' and fictitious air enthalpy ' h_{ref} ' at refrigerant temperature. However, arithmetic enthalpy difference does not account for variation in air enthalpy. Hence, arithmetic enthalpy difference is replaced by logarithmic enthalpy difference to consider the variation in air enthalpy (Threlkeld, 1970f):

$$dQ_{node} = U_o a_{node} \times \Delta h = U_o a_{node} \times \frac{h_{a,in} - h_{a,ex}}{\log \frac{h_{a,in} - h_{ref}}{h_{a,ex} - h_{ref}}} \quad (17)$$

Under wet surface condition, the correlation proposed by Nuntaphan et al. (2005) is used to calculate air side heat transfer coefficient and pressure drop. The convective heat transfer coefficient for the refrigerant in two phase region is estimated using the correlation proposed by Yoon et al. (2004); while the convective heat transfer coefficient for the refrigerant in single phase vapor zone is estimated using the correlation proposed by Gnielinski (Pitla et al., 2002b).

Table 1: Dimensions predicted for heat exchangers

Tube			Fin		
Parameter	Gas cooler	Evaporator	Parameter	Gas cooler	Evaporator
Material	Copper	Copper	Material	Copper	Copper
Inner diameter	5.5 mm	5.5 mm	Outer diameter	26 mm	26 mm
Outer diameter	9.5 mm	9.5 mm	Fin thickness	0.19 mm	0.19 mm
Longitudinal tube pitch (P_l)	30 mm	30 mm	Fin pitch	3 mm	4 mm
Transverse tube pitch (P_t)	27 mm	30 mm			
Parameter		Gas cooler	Evaporator		
Finning length of tube		480 mm	300 mm		
Number of tubes in each row		18	13		
Number of tube rows		3	3		
Total fin surface area		8.0837 m ²	2.7367 m ²		
Unfinned base surface area		0.7243 m ²	0.3324 m ²		
Total surface area		8.8080 m ²	3.0691 m ²		

Table 2: Standard operating parameters considered for carrying out the simulation

Parameter	Value
High side pressure in gas cooler	100 bar
Superheat at compressor inlet	5°C
Displacement volume of compressor at 1450 rpm	1.05 m ³ /hr
Temperature of air supplied to gas cooler	35°C
DBT and RH of air supplied to evaporator	25°C and 60%

4. RESULTS AND DISCUSSIONS

Based on the model described above, an in-house code has been developed on the MATLAB platform. To evaluate the thermodynamic properties of CO₂, REFPROP 9 is integrated with the MATLAB code. The flowchart of the developed model is shown in figure 6. While designing the gas cooler and evaporator; number of tube rows, tube diameter, tube thickness, tube pitch, length of tube in each row, fin diameter, fin thickness, and fin pitch are entered as input values. Finally the number of tubes in each row is calculated by an iterative procedure. Criterion for iterative procedure is required heat transfer rate. Table 1 shows the predicted dimensions for gas cooler and evaporator. Also numerical simulations are carried out using the developed model, to investigate the effect of variation in high side pressure in the gas cooler and ambient conditions on the performance of the system. High side pressure is varied from 95 bar to 115 bar. Temperature of ambient air supplied to the gas cooler is varied from 33°C to 39°C. While, DBT of air supplied to the evaporator is varied from 23°C to 28°C. The standard operating

parameters are shown in table 2. Optimum operating parameters at which the system attains maximum COP are identified from numerical simulations and are presented in table 3.

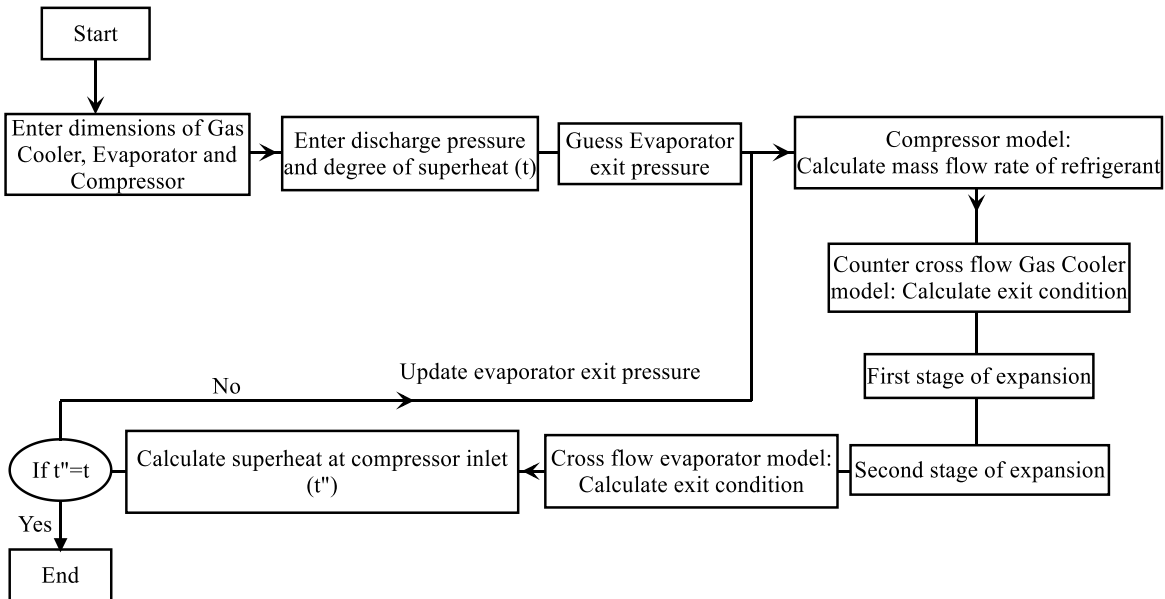


Figure 6: Flowchart of the developed model for R744 based air conditioning cycle

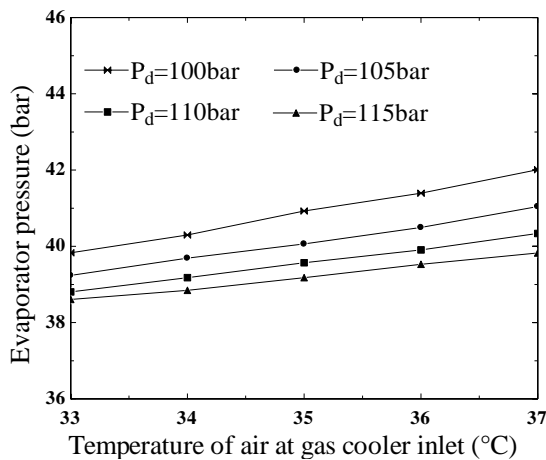


Figure 7: Variation of evaporator pressure with change in temperature at gas cooler inlet

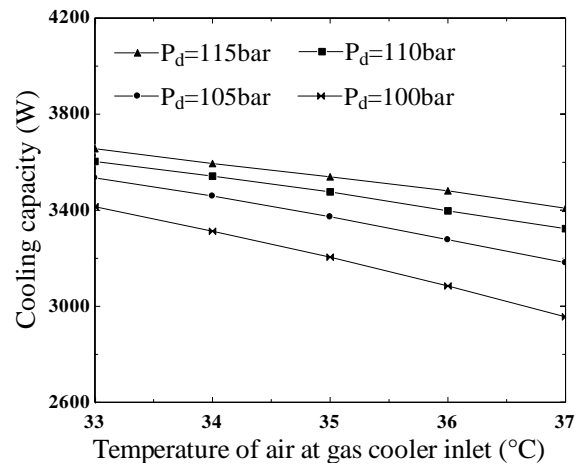


Figure 8: Variation of evaporator capacity with change in temperature at gas cooler inlet

4.1 Effect of variation in ambient temperature

With increase in temperature of air supplied to the gas cooler, evaporator pressure is observed to increase (figure 7). Evaporator capacity decreases with increase in ambient temperature (figure 8), while compressor power remains almost constant (figure 9). COP exhibits a decrease with increase in ambient temperature (figure 10). With increase in temperature of air supplied to gas cooler, quality of refrigerant at evaporator inlet deteriorates. Therefore, requirement of refrigerant flow rate through evaporator increases to produce the required amount of superheat. To fulfil the requirement of higher flow rate through evaporator, evaporator pressure goes up and compressor volumetric efficiency increases. Thus suction of total refrigerant flow rate to the compressor increases. As the system is supposed to run at a fixed discharge pressure, pressure ratio decreases with increase in evaporator pressure. However, rate of decrement in pressure ratio is balanced by the rate of increment in mass flow rate. Hence, power requirement to drive the compressor remains almost constant. However evaporator capacity decreases continuously. As a result COP is found decreasing with increase in temperature of air supplied to the gas cooler.

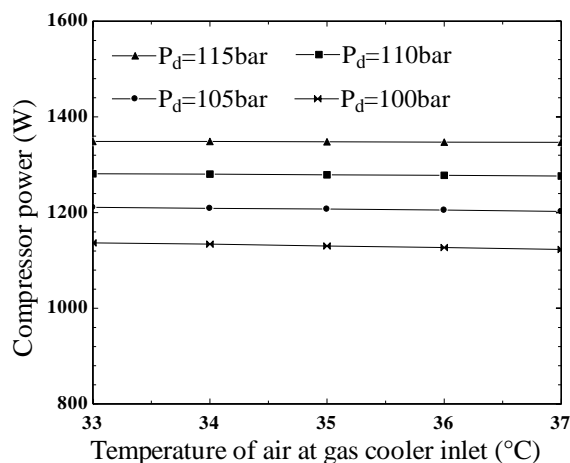


Figure 9: Variation of compressor power with change in temperature at gas cooler inlet

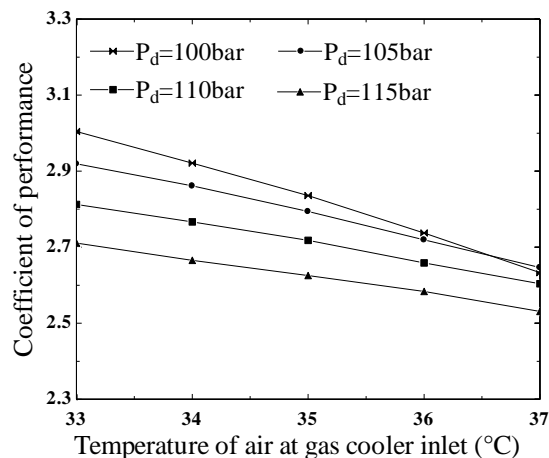


Figure 10: Variation of COP with change in temperature at gas cooler inlet

For a constant ambient temperature, with increase in discharge pressure, refrigerant quality at the inlet of evaporator improves. As a result, requirement of refrigerant flow rate reduces to produce the required amount of superheat. Hence evaporator pressure decreases. As the system is supposed to run at fixed discharge pressure, pressure ratio decreases and hence volumetric efficiency also decreases with decrease in evaporator pressure. Mass flow rate of refrigerant decreases as volumetric efficiency decreases. With increase in pressure ratio, power required to drive the compressor increases. Cooling capacity also increases with increase in discharge pressure. COP is found increasing for the cases for which rate of increment in cooling capacity is more compared to the rate of increment in compressor power.

Table 3: Predicted optimum discharge pressure for system with double stage expansion

Ambient temperature (°C)	Performance of system with double stage expansion			
	Optimum discharge pressure (bar)	Differential pressure drop (bar)	Cooling capacity (W)	System COP
33	95	20.97	3205.8	3.04
34	95	20.33	3067.8	2.92
35	100	26.07	3204.5	2.84
36	100	25.48	3084.4	2.74
37	105	31.00	3182.0	2.65
38	105	30.49	3074.7	2.57
39	110	35.86	3146.1	2.47

4.2 Effect of variation in DBT of air supplied to evaporator

The effects of changes in DBT of air supplied to the evaporator on system performance are analyzed here. Both evaporator pressure and evaporator capacity have been found increasing with increase in DBT of air (figure 11). Power required for driving the compressor decreases while COP increases with increase in DBT of air (figure 12). With increase in DBT of air, temperature difference between air and refrigerant increases. As a result, requirement of refrigerant flow rate increases to produce the desirable amount of superheat. That is why evaporator pressure goes up, volumetric efficiency of compressor increases and suction of refrigerant flow rate to the compressor increases. As the system is supposed to run at constant discharge pressure, pressure ratio decreases with increase in evaporator pressure. Hence power requirement to drive the compressor decreases. Since evaporator capacity increases, COP improves with increase in DBT of air supplied to the evaporator.

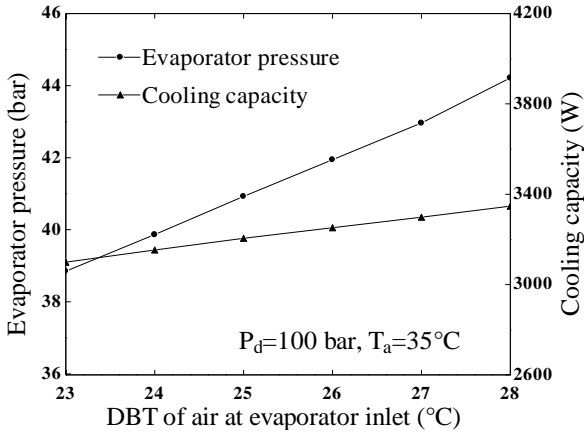


Figure 11: Variation of evaporator pressure and cooling capacity with changes in DBT of air at evaporator inlet

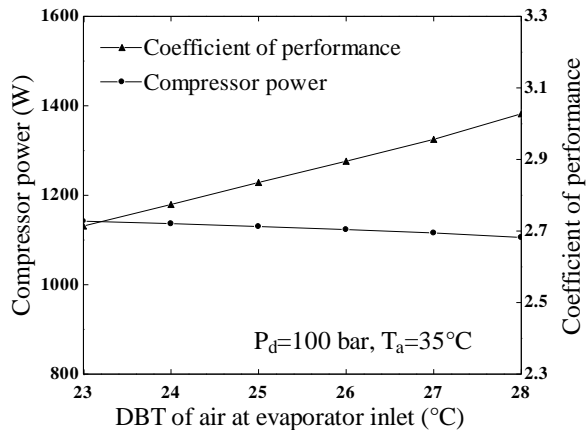


Figure 12: Variation of compressor power and COP with changes in DBT of air at evaporator inlet

5. CONCLUSIONS

An R744 based air conditioning cycle considered here employs two expansion valves. For this proposed cycle, a comprehensive mathematical model has been developed. Fin and tube heat exchangers employed are modelled based on a discretized approach. The developed model is subsequently used to predict the dimensions for all components. Numerical simulations are also carried out using the model for the R744 based air conditioning cycle. From the results obtained, the effects of variation of various important environmental parameters on system performance are analyzed. For a discharge pressure of 100 bar, when temperature of air supplied to the gas cooler is varied from 33°C to 37°C, system COP reduces by 12.3% from 3.00 to 2.63. On the other hand, when DBT of air supplied to the evaporator is varied from 23°C to 28°C, system COP increases by 11.8% from 2.71 to 3.03. Finally, optimum operating conditions are identified for which the system attains maximum COP based on the results of numerical simulations.

NOMENCLATURE

W	Power (W)	m	Mass flow rate (kg/s)
h	Specific enthalpy (J/kg)	r_p	Pressure ratio
PD	Displacement volume (m^3/s)	Q	Heat transfer rate (W)
P	Pressure (Pa)	T	Temperature (K)
L	Length of each tube (m)	d	Diameter (m)
a_{node}	Surface area of each elementary node (m^2)	r	Radius (m)
G	Mass flux (kg/m^2s)	U	Universal heat transfer coefficient (W/m^2K)
y_w	Water film thickness (m)	b	Slope of saturated air enthalpy
k	Thermal conductivity (W/mK)	C_p	Specific heat (J/kgK)
w	Specific humidity ratio (kg of w.v./kg of d.a.)	f	Fanning friction factor

Greek symbol

η	Efficiency	ρ	Density
α	Heat transfer coefficient (W/m^2K)		

Superscript and subscript

com	Compressor	ref	Refrigerant
a	Air	w	Water
is	Isentropic	v	Volumetric
in	Inlet	ex	Exit

<i>i</i>	Inner	<i>o</i>	Outer
<i>f</i>	Fin	<i>s</i>	Tube surface
<i>d</i>	Compressor discharge		

Abbreviation

RPS	Revolution per second	COP	Coefficient of performance
LMTD	Log mean temperature difference	DBT	Dry bulb temperature
RH	Relative humidity	DPT	Dew point temperature

REFERENCES

- Boccardi, G., Calabrese, N., Celata, G. P., Mastrullo, R., Mauro, A. W., Perrone, A., Trinchieri, R. (2013). Experimental performance evaluation for a carbon dioxide light commercial cooling application under transcritical and subcritical conditions. *Applied Thermal Engg.*, 54, 528-35.
- Brown, J. S., Yana-Motta, S. F., Domanski, P. A. (2002). Comparative analysis of an automotive air conditioning systems operating with CO₂ and R134a. *Int. J. Refrig.*, 25, 19–32.
- Casson, V., Cecchinato, L., Corradi, M., Fornasieri, E., Giroto, S., Minetto, S., Zamboni, L., Zilio, C. (2003). Optimisation of the throttling system in a CO₂ refrigerating machine. *Int. J. Refrig.*, 26, 926–35.
- Elbel, S., Fuentes, Y. P., Bowers, C. D., Hrnjak, P. S. (2014). Successful design, implementation, and validation of Transcritical R744 technology for beverage display coolers. *Int. Refrig. & Air Cond. Conf.*, Purdue University.
- Lorentzen, G., Pettersen, J. (1993). A new, efficient and environmentally benign system for car air-conditioning. *Int. J. Refrig.*, 16., 4–12.
- Nuntaphan, A., Kiatsiriroat, T., Wang, C. C. (2005). Heat transfer and friction characteristics of crimped spiral finned heat exchangers with dehumidification. *Applied Thermal Engg.*, 25, 327–40.
- Peñarocha, I., Llopis, R., Tárrega, L., Sánchez, D., Cabello, R. (2014). A new approach to optimize the energy efficiency of CO₂ transcritical refrigeration plants. *Applied Thermal Engg.*, 67, 137-46.
- Pitla, S. S., Groll, E. A., Ramadhyani, S. (2002). New correlation to predict the heat transfer coefficient during in-tube cooling of turbulent supercritical CO₂. *Int. J. of Refrig.*, 25(7), 887-95.
- Pongsoi, P., Promoppatum, P., Pikulkajorn, S., Wongwises, S. (2013). Effect of fin pitches on the air-side performance of L-footed spiral fin-and-tube heat exchangers. *Int. J. of Heat Mass Transfer*, 59, 75–82.
- Threlkeld, J. L. (1970). *Thermal Environmental Engineering*, Prentice-Hall, Inc., New York, NY.
- Yin, J. M., Bullard, C. B., Hrnjak, P. S. (2001). R-744 gas cooler model development and validation, *Int. J. Refrig.*, 24(7), 692-701.
- Yoon, S. H., Cho, E. S., Hwang, Y. W., Kim, M. S., Min, K., Kim, Y. (2004). Characteristics of evaporative heat transfer and pressure drop of carbon dioxide and correlation development. *Int. J. Refrig.*, 27, 111–19.
- Zhang, X. P., Fan, X. W., Wang, F. K., Shen, H. G. (2010). Theoretical and experimental studies on optimum heat rejection pressure for a CO₂ heat pump system. *Applied Thermal Engg.*, 30., 2537-44.

ACKNOWLEDGEMENT

The work is supported by Science and Engineering Research Board (SERB), Technology Bhawan, New Mehrauli Road, New Delhi, for the project *Design and development of a demonstration unit of carbon dioxide based transcritical refrigeration system*.